Received: 21 June 2023 | Accepted: 31 July 2023

DOI: 10.1097/HEP.0000000000000568

ORIGINAL ARTICLE

OPEN

Metabolic reprogramming in Nrf2-driven proliferation of normal rat hepatocytes

Marta A. Kowalik[1] | Keiko Taguchi[2,3] | Marina Serra[1] | Andrea Caddeo[1] | Elisabetta Puliga[4,5] | Marina Bacci[6] | Seizo Koshiba[2,3] | Jin Inoue[2,3] | Eiji Hishinuma[2,3] | Andrea Morandi[6] | Silvia Giordano[4,5] | Andrea Perra[1] | Masayuki Yamamoto[2,3] | Amedeo Columbano[1]

[1]Department of Biomedical Sciences, Unit of Oncology and Molecular Pathology, University of Cagliari, Cagliari, Italy

[2]Department of Molecular Biology and Biochemistry, Tohoku Medical Megabank Organization, Tohoku University, Sendai, Japan

[3]Advanced Research Center for Innovations in Next Generation Medicine (INGEM), Tohoku University, Sendai, Japan

[4]Department of Oncology, University of Torino, Candiolo, Italy

[5]Department of Oncology Candiolo Cancer Institute, FPO-IRCCS, Candiolo, Torino, Italy

[6]Department of Experimental and Clinical Biomedical Sciences, University of Firenze, Florence, Italy

Correspondence
Amedeo Columbano, Department of Biomedical Sciences, Unit of Oncology and Molecular Pathology, University of Cagliari, Cittadella Universitaria, SP. 8 Monserrato, 09042 Monserrato, Italy.
Email: columbano@unica.it

Masayuki Yamamoto, Department of Molecular Biology and Biochemistry, Tohoku Medical Megabank Organization, Tohoku University, Sendai 980-8573, Japan.
Email: masiyamamoto@med.tohoku.ac.jp

Abstract

Background and Aims: Cancer cells reprogram their metabolic pathways to support bioenergetic and biosynthetic needs and to maintain their redox balance. In several human tumors, the Keap1-Nrf2 system controls proliferation and metabolic reprogramming by regulating the pentose phosphate pathway (PPP). However, whether this metabolic reprogramming also occurs in normal proliferating cells is unclear.

Approach and Results: To define the metabolic phenotype in normal proliferating hepatocytes, we induced cell proliferation in the liver by 3 distinct stimuli: liver regeneration by partial hepatectomy and hepatic hyperplasia induced by 2 direct mitogens: lead nitrate (LN) or triiodothyronine. Following LN treatment, well-established features of cancer metabolic reprogramming, including enhanced glycolysis, oxidative PPP, nucleic acid synthesis, NAD^+/NADH synthesis, and altered amino acid content, as well as downregulated oxidative phosphorylation, occurred in normal proliferating hepatocytes displaying Nrf2 activation. Genetic deletion of Nrf2 blunted LN-induced PPP activation and suppressed hepatocyte proliferation. Moreover, Nrf2 activation and following metabolic reprogramming did not occur when hepatocyte proliferation was induced by partial hepatectomy or triiodothyronine.

Conclusions: Many metabolic changes in cancer cells are shared by proliferating normal hepatocytes in response to a hostile environment. Nrf2

Abbreviations: Aldh18a1, aldehyde dehydrogenase 18 family member A1; BR, brusatol; BrdU, bromodeoxyuridine; G6pc, glucose-6-phosphatase; G6PD, glucose-6-phosphate dehydrogenase; Gclc, glutamate-cysteine ligase catalytic subunit; Glud1, glutamate dehydrogenase 1; Glul, glutamate-ammonia ligase; Glut1, glucose transporter-1; Gs, glutamine synthetase; Gstp1, placental glutathione S-transferase; Idh1, isocitrate dehydrogenase 1; IHC, immunohistochemistry; Keap1, kelch-like ECH-associated protein 1; KO, knockout; LN, lead nitrate; Mct4, monocarboxylate transporter 4; Me1, malic enzyme 1; Nqo1, NAD(P)H quinone dehydrogenase 1; Nrf2, nuclear factor (erythroid-derived 2)-like 2; OXPHOS, oxidative phosphorylation; p62, sequestosome; Pgd, phosphogluconate dehydrogenase; PH, partial hepatectomy; PPP, pentose phosphate pathway; Prodh, proline dehydrogenase; Pycr1, pyrrolidine-5-carboxylate reductase; qRT-PCR, quantitative reverse transcriptase PCR; T3, triiodothyronine; TCA, tricarboxylic acid cycle; WT, wild-type.

Marta A. Kowalik and Keiko Taguchi equally contributed to the work. Andrea Caddeo is a recipient of the Fondazione Umberto Veronesi Fellowship.

Supplemental Digital Content is available for this article. Direct URL citations are provided in the HTML and PDF versions of this article on the journal's website, www.hepjournal.com.

activation is essential for bridging metabolic changes with crucial components of cancer metabolic reprogramming, including the activation of oxidative PPP. Our study demonstrates that matured hepatocytes exposed to LN undergo cancer-like metabolic reprogramming and offers a rapid and useful *in vivo* model to study the molecular alterations underpinning the differences/similarities of metabolic changes in normal and neoplastic hepatocytes.

INTRODUCTION

Cancer develops through a multistep process in which neoplastic cells acquire several functional traits, the so-called "hallmarks of cancer," which allows them to proliferate, survive, and disseminate.[1] Metabolic reprogramming is an established hallmark of cancer.[2] Unlike normal cells, neoplastic cells demonstrate a distinctive form of cellular metabolism and undergo an important metabolic shift, called the Warburg effect,[3] in which glucose utilization is favored and oxidative phosphorylation (OXPHOS) is often impaired, thus providing rapidly dividing tumor cells with metabolic intermediates that serve as biosynthetic precursors.[4]

However, the last decades of research have shown that cancer metabolic reprogramming is much more complex. In this context, the Kelch-like ECH associated protein 1/nuclear factor erythroid-derived 2-like 2 (Keap1-Nrf2) system, the main intracellular defense against environmental stress,[5] has been recognized as an important regulator of proliferation and metabolic reprogramming in several human tumors.[6] Nrf2 activation increases glucose uptake and directs it to the pentose phosphate pathway (PPP) by regulating the expression of the key enzymes involved in the oxidative and nonoxidative branches of the PPP.[7] Numerous studies reported that Nrf2 activation through different mechanisms is frequently observed in primary tumors and sustains cancer progression (reviewed in Menegon et al[8]).

Both metabolic reprogramming and Nrf2 activation characterize HCC, one of the most frequent and lethal human cancers.[9] Indeed, whole-exome sequencing and the Cancer Genome Atlas–derived data revealed mutations of either *NRF2* (6.4%) or *KEAP1* (2%–11%),[10,11] as well as other KEAP1-NRF2 alterations in 19% of HCCs.[12] As previously reported, the Warburg effect is an early event in rat hepatocarcinogenesis, identifies a subset of aggressive preneoplastic lesions, and is maintained in advanced HCC.[13,14] Importantly, Nrf2 induces the expression of glucose-6-phosphate dehydrogenase (G6PD), the rate-limiting enzyme of the PPP, required to support the anabolic demands and orchestrate metabolic deregulation.[7] In agreement, metabolic changes leading to increased G6PD expression are associated with a higher proliferative capacity of preneoplastic lesions.[13] Although the liver is the central metabolic organ that orchestrates the interplay of multiple metabolic processes, no in-depth studies have been undertaken to assess whether normal hepatocytes undergo metabolic reprogramming, like that observed in cancer cells, when stimulated to proliferate.

So far, only few studies explored the role of Nrf2 in normal hepatocyte proliferation. A delay of the regenerative process was observed in Nrf2-lacking mice after two-thirds of partial hepatectomy (PH),[15,16] the best recognized experimental model of rapid, controlled, and reproducible cell proliferation in a mammalian organ system.[17,18] Oddly enough, a delay in liver regeneration after PH was observed also in mice bearing a constitutively active Nrf2[19] and in Nrf2 overexpressing *Keap1*$^{+/-}$ mice.[20] Thus, whether Nrf2 activation is a *sine qua non* condition for appropriate liver regeneration remains unknown. This is a relevant question as an efficient regenerative ability of the liver is required in conditions such as the transplantation of partial liver grafts and living-related transplantation or in the elderly status characterized by an impaired liver regenerative capacity.[21]

Differentiated hepatocytes are induced to proliferate not only after cell death/loss but also following treatment with primary mitogens that can induce the entry of hepatocytes into the cell cycle in the absence of cell death.[22] Among these mitogens, lead nitrate (LN) is particularly interesting as hepatocyte proliferation induced by this metal salt was not associated with any significant changes in the hepatic levels of HGF, TGF-α, or TGF-β1 mRNA, usually associated with liver regeneration.[23] Instead, LN-induced liver cell proliferation resulted in a rapid increase of hepatic expression of TNF-α mRNA, suggesting that TNF-α is involved in triggering LN-induced hepatocyte proliferation. Accordingly, inhibition of TNF-α expression blunted LN-induced hepatocyte proliferation.[24] Notably, unlike other hepatomitogens, repeated rounds of cell proliferation caused by LN did not promote diethylnitrosamine-induced HCC development.[25]

By using 3 distinct protocols of hepatocyte proliferation, namely, (1) liver regeneration following PH, (2) direct hyperplasia induced by the mitogens LN, or (3) triiodothyronine (T3), we investigated whether (1) Nrf2

activation is mandatory for the entry into cell cycle of differentiated hepatocytes, (2) Nrf2 activation is required for the induction of metabolic reprogramming in normal proliferating hepatocytes, and (3) metabolic reprogramming similar to that observed in preneoplastic and neoplastic hepatocytes occurs in proliferating normal hepatocytes.

METHODS

Rats and treatment

PH was performed according to Higgins and Anderson.[17] LN dissolved in distilled water was injected through the femoral vein at a single dose of 10 μmol/100 g body weight. T3 was given as a single i.p. dose at 20 μg/100 g body weight. Rats were killed 24, 48, and 72 hours and 10 days after treatment with PH, LN, or T3. All rats received bromodeoxyuridine (BrdU, 1 mg/mL) in drinking water for 24 hours prior to sacrifice. Brusatol (0.5 mg/kg body weight) was injected intraperitoneally 2 hours after LN injection. Rats were killed 48 hours after LN treatment. All procedures were performed in male F-344 rats in accordance with the Guidelines for the Care and Use of Laboratory Animals.

Nrf2 knockout (KO)[26] and wild-type (WT) rats were injected with LN or T3 as described previously. Animal procedures were performed according to The Standards for Human Care and Use of Laboratory Animals of Tohoku University and Guidelines for Proper Conduct of Animal Experiments of the Ministry of Education, Culture, Sports, Science, and Technology of Japan.

Histology and immunohistochemistry

Sections of the liver were processed for staining with hematoxylin-eosin or immunohistochemistry (IHC) or snap-frozen in liquid nitrogen and used for histochemistry. BrdU detection was performed as described.[14] For details, see Supplemental Material, http://links.lww.com/HEP/I5 and Supplemental Table S1, http://links.lww.com/HEP/I5.

RNA extraction and quantitative reverse transcription PCR analysis

Total RNA was extracted from 50–100 mg of frozen liver from rats treated with LN, PH, or T3 and quantified with NanoDrop. RNA (2 μg) was reverse-transcribed using High-Capacity cDNA Reverse Transcription Kit. The mRNA expression was assessed by quantitative reverse transcription PCR (qRT-PCR) analysis using 10 ng of cDNA mixed with 2X TaqMan Gene expression Master Mix and 20X specific TaqMan gene expression assays with an ABI PRISM 7300 Thermocycler. qRT-PCR primers used were listed in Supplemental Table S2, http://links.lww.com/HEP/I5. Gene expression analysis of *Gapdh* was used as an endogenous control. Relative quantification for each gene was calculated by the $2^{-\Delta\Delta Ct}$ method.

Western blot

Western blot was performed according to standard methods. The primary antibodies used were listed in Supplemental Table S1, http://links.lww.com/HEP/I5.

Metabolome analyses

Rat liver tissue was homogenized using a Precellys 24 bead-based homogenizer with zirconium oxide beads (M&S Instruments Inc., Osaka, Japan) by adding 300 μL of cold methanol per 100 mg of liver tissue. For details, see Supplemental Material, http://links.lww.com/HEP/I5 and Koshiba et al.[27]

Complex II/succinate dehydrogenase histochemical assay and measurement of enzymatic activity of mitochondrial complex II

The enzymatic assay was performed as described.[13] For further details on the measurement of enzymatic activity of mitochondrial complex II, see Supplemental Material, http://links.lww.com/HEP/I5.

Statistical analysis

All data were expressed as the mean ± SD or the mean ± SEM. Differences between groups were compared using Student *t* test or ANOVA with the use of GraphPad Software Inc. (San Diego, CA). A value of $p < 0.05$ was considered a significant difference between groups.

RESULTS

Nrf2 activation occurs in LN- but not in T3- or PH-induced hepatocyte proliferation

The extent and kinetics of hepatocyte proliferation were investigated in rats at 24, 48, and 72 hours and 10 days after treatment with a single dose of 2 direct mitogens: LN and T3. Cellular proliferation was assessed by BrdU incorporation. Hepatocytes, in addition to nonparenchymal cells, proliferated in LN-treated rats at 48 hours (Figure 1A,

upper panels), while only hepatocytes were BrdU-positive following T3 treatment (Figure 1A, lower panels).

Quantification of hepatocyte proliferation showed a peak at 48 hours after the challenge of LN or T3 (Figure 1B), associated with an increased mitotic index (Figure 1C) compared to controls. A complete return to quiescence was observed 10 days after the proliferative stimuli (Figure 1B, C). In agreement with previous studies,[18] we observed increased hepatocyte proliferation after PH with a peak at 24 hours and a return to quiescence 10 days after surgery (Supplemental Figure S1A, http://links.lww.com/HEP/I6).

LN, but not T3 and PH, activates Nrf2 and induces the expression of Nrf2 target genes

To investigate whether Nrf2 is involved in hepatocyte proliferation, by qRT-PCR analysis, we evaluated the expression of 3 well-characterized Nrf2 target genes,[7] ie, NAD(P)H quinone dehydrogenase 1 (*Nqo1*), glutathione *S*-transferase 1 (*Gstp1*), and glutamate-cysteine ligase catalytic subunit (*Gclc*). Of note, a very strong increase in *Nqo1, Gclc,* and *Gstp1* mRNA levels was observed 24 and 48 hours after LN (Figure 2A). In contrast, mRNA levels of *Nqo1*, *Gstp1*, *and Gclc* were not induced substantially in T3-induced hepatocyte proliferation or during liver regeneration following PH, despite a massive hepatocyte proliferation (Figure 1B).

The expression of these Nrf2 target genes was almost normalized 10 days after LN, T3, and PH (Figure 2A) concomitantly with the return of hepatocytes to a quiescent state in Figure 1B, C. IHC analysis confirmed these results, showing that almost all hepatocytes were positive for NQO1 and GSTP in LN-treated rats at 48 hours, whereas they were virtually negative in rats treated with T3 or PH (Figure 2B). Overall, these results indicate that Nrf2 activation occurs in LN-induced hepatocyte proliferation, while it is not required for entry into the cell cycle following T3 or PH.

LN induces p62 accumulation and phosphorylation

Next, we investigated the possible mechanism(s) underlying LN-induced Nrf2 activation. The comparable levels of *Keap1* mRNA in controls and LN-treated rats after 24 hours to 10 days (Figure 2C) ruled out that a decreased *Keap1* transcription could be responsible for the enhanced Nrf2 activation. Among several modalities of Nrf2 activation, we explored the possibility that a "noncanonical" regulation of the Keap1-Nrf2 system mediated by the selective autophagy adaptor p62, also known as sequestosome 1 and A170 (p62/SQSTM1/A170), could act in this context.[28,29] As shown in

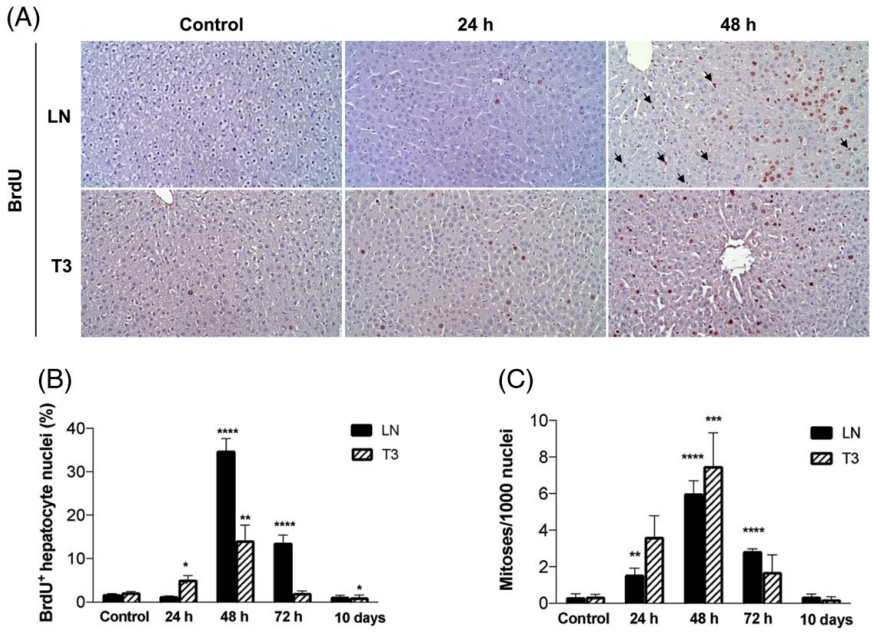

FIGURE 1 Both LN and T3 induce hepatocyte proliferation. (A) Microphotograph showing BrdU-positive nuclei in the liver of rats 24 and 48 hours after treatment with LN (100 μmol/100 g body weight) or T3 (20 μg/100 g body weight). Arrows indicate nonparenchymal cells (hematoxylin-eosin; ×20 magnification). (B) Labeling index (LI) of hepatocytes 24, 48, and 72 hours and 10 days after treatment of LN or T3. BrdU (1 mg/mL) dissolved in drinking water was given for 24 hours before sacrifice. LI was expressed as the number of BrdU-positive hepatocyte nuclei/100 nuclei. (C) Mitotic index (MI) of hepatocytes in rats treated as in A. MI was expressed as the number of mitoses/1000 hepatocyte nuclei. Each bar represents the mean ± SD of 3 to 5 samples per group. *$p < 0.05$, **$p < 0.01$, ***$p < 0.001$, and ****$p < 0.0001$ compared to its control. Abbreviations: BrdU, bromodeoxyuridine; LN, lead nitrate; T3, triiodothyronine.

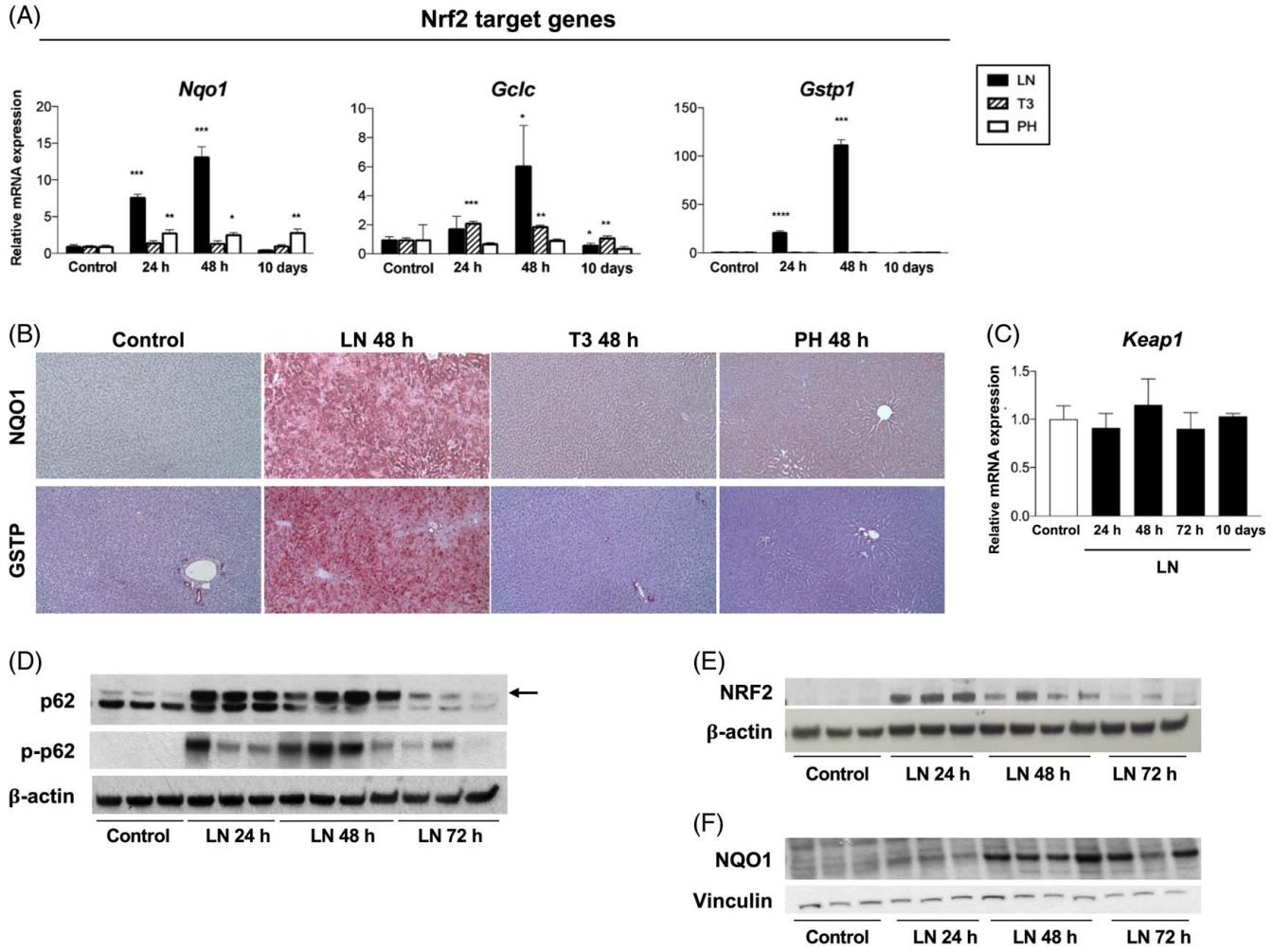

FIGURE 2 LN, but not T3 and PH, activates Nrf2 and induces the expression of Nrf2 target genes and p62 accumulation. (A) qRT-PCR analysis of *Nqo1*, *Gclc*, and *Gstp1* mRNA expression levels in the liver at 24 and 48 hours and 10 days after treatment with three different proliferative stimuli. Gene expression is reported as fold-change relative to livers from control rats. The graph bar represents the mean ± SD of 5–6 rats/group (*t* test). *$p < 0.05$, **$p < 0.01$, *** $p < 0.001$, and ****$p < 0.0001$ compared to its own control. (B) IHC analysis of NQO1 and GSTP in livers (×10 magnification) 48 hours after treatment with LN, T3, or PH. (C) qRT-PCR analysis of *Keap1* mRNA expression level in the liver of control or LN-treated rats at 24 and 48 hours and 10 days. Relative mRNA expression was calculated using *Gapdh* as an endogenous control. Gene expression is reported as fold-change relative to livers from control rats. Each bar represents the mean ± SD of 3–5 samples per group. Western blot analysis showing p62 and phospho-p62 (D), NRF2 (E), and NQO1 (F) in the liver of control rats and LN-treated rats for 24, 48, and 72 hours. β-actin was used as a housekeeper protein. Abbreviations: Gclc, glutamate-cysteine ligase catalytic subunit; Gstp1, placental glutathione S-transferase; Keap1, kelch-like ECH-associated protein 1; LN, lead nitrate; Nqo1, NAD(P)H quinone dehydrogenase 1; Nrf2, nuclear factor (erythroid-derived 2)-like 2; PH, partial hepatectomy; T3, triiodothyronine.

Figure 2D, western blot analysis revealed p62 accumulation in LN-treated compared to rat control liver (Figure 2D). As expected, p62 was phosphorylated at Ser 351 in LN-treated liver at 24–48 hours. Simultaneously, Nrf2 and Nqo1 accumulated in LN-treated livers, with a peak at 24–48 and 48–72 hours, respectively (Figure 2E, F). Thus, enhanced phosphorylation and massive accumulation of p62 seem to be responsible for the increased Nrf2 accumulation.

LN enhances PPP activation

Nrf2 plays a crucial role in redirecting cancer cell metabolism toward glucose consumption and PPP activation.[7] However, it is unknown whether Nrf2 activation in normal proliferating hepatocytes induces a similar metabolic rewiring. To address this question, we analyzed the expression of genes encoding PPP enzymes. A highly significant increase in the expression of *G6pd*, the key limiting enzyme of the PPP oxidative branch, was observed after LN but not T3 (Figure 3A). Consistently, IHC showed a marked increase of G6PD levels in hepatocytes after 48 hours of LN treatment, but not after 48 hours of T3 treatment (Figure 3B). No evidence of different G6PD protein levels was observed after PH as demonstrated by IHC (Supplemental Figure S1B, http://links.lww.com/HEP/I6) and previous studies.[13] Conversely, the expression of Tkt, encoding for a key enzyme of the nonoxidative branch of PPP, was

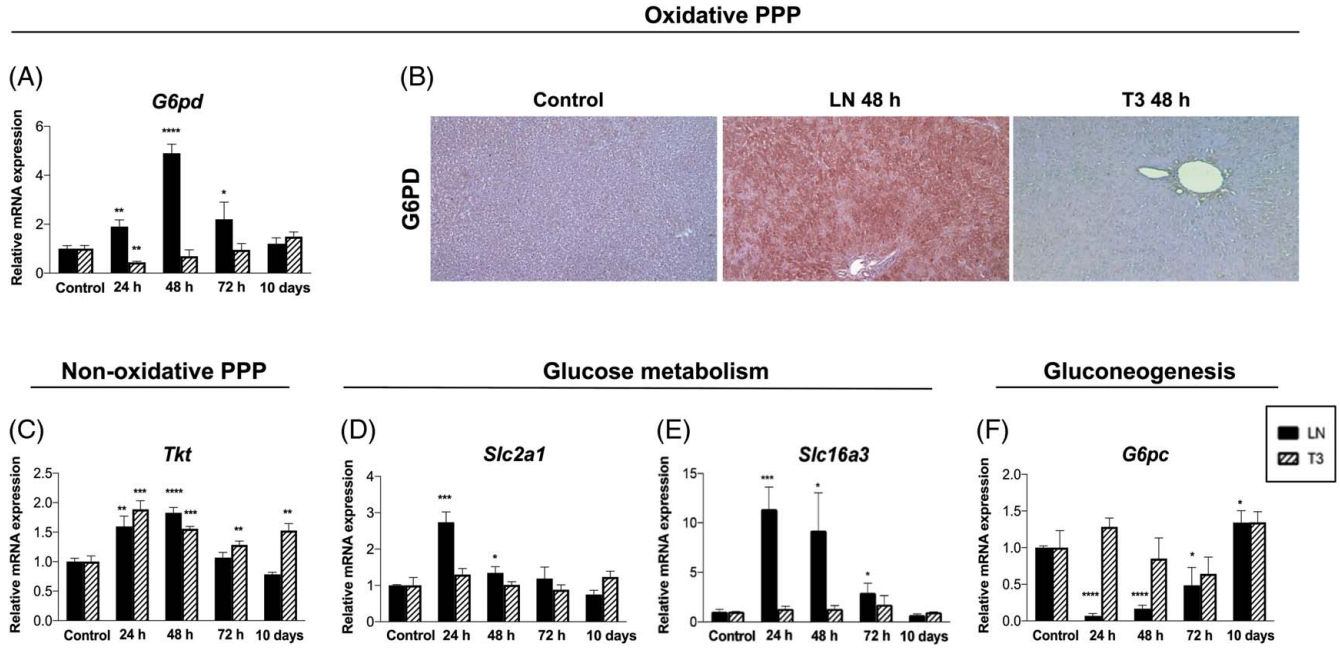

FIGURE 3 LN, but not T3, induces PPP and glycolysis. qRT-PCR (A) and IHC analysis (B) of G6PD in livers (×10 magnification) from rats treated with LN or T3. qRT-PCR analysis of *Tkt* (C), and glycolysis-related genes, such as *Slc2a1* (D), *Slc16a3* (E), and *G6pc* (F) in the livers of control rats, and the rats at 24, 48, and 72 hours and 10 days after treatment with LN or T3. Relative mRNA expression was calculated using *Gapdh* as an endogenous control. Gene expression is reported as fold-change relative to livers from control rats. The graph bar represents mean values ± SD of 3–5 rats/group (*t* test). *$p < 0.05$, **$p < 0.01$, *** $p < 0.001$, and ****$p < 0.0001$ compared to its own control. Abbreviations: G6pc, glucose-6-phosphatase; G6PD, glucose-6-phosphate dehydrogenase; LN, lead nitrate; PPP, pentose phosphate pathway; T3, triiodothyronine.

moderately but significantly induced upon both LN and T3 administration (Figure 3C).

Notably, the mRNA levels of the glucose transporter-1 (*Glut1*, *Slc2a1*) and the lactate extruder *Slc16a3* (monocarboxylate transporter 4, Mct4), involved in glucose metabolism, rapidly increased following LN, but not T3 treatment (Figure 3D, E) or PH (Supplemental Figure S1C, http://links.lww.com/HEP/I6). On the contrary, the expression of *G6pc,* an enzyme involved in gluconeogenesis, was severely downregulated in LN-treated livers at all-time points (Figure 3F).

LN redirects glutamine metabolism toward glutamate

In cancer-related metabolic reprogramming, Nrf2 has been shown to stimulate changes in glutamine metabolism.[7] Therefore, we wished to determine the relevance of glutamine in proliferating hepatocytes carrying Nrf2 activation. IHC analysis revealed that, in control livers glutamine synthetase (GS), the enzyme that catalyzes the conversion of glutamate into glutamine was present in the hepatocytes surrounding the terminal hepatic venules, while, in the livers of LN-treated rats, GS staining was limited only to the first rim of hepatocytes (Figure 4A). Further analysis revealed that the reduction of GS (*Glul* gene) after treatment with LN was the consequence of the significant reduction of the mRNA levels (Figure 4B).

GS is a direct target of activated β-catenin that is frequently mutated and overexpressed in human and rodent HCCs.[30,31] However, the possibility that the reduced expression of GS could be due to β-catenin downregulation was excluded since livers from 48 hours LN-treated rats displayed a strong β-catenin accumulation (Figure 4C).

Interestingly, metabolomics performed on LN-treated hepatocytes revealed a decrease of glutamine compared to the control liver, concomitant with a striking increase of glutamate and glycine (Figure 4D). This observation is in agreement with the metabolome results from Nrf2-activated cancer cells.[7] As shown in Figure 2A, Nrf2 promotes transcription of *Gclc*, a rate-limiting enzyme of glutathione biosynthesis.[32] Indeed, glycine and glutathione content strongly increased following the LN treatment (Figure 4D), implying that LN treatment induces glutathione synthesis through Nrf2 induction.

Glutamate dehydrogenase 1 (*Glud1*) mRNA level was decreased in the liver of LN-treated rats at 24 hours (Figure 4E), concomitant with the increase of *Gclc* mRNA (Figure 2A). The significant decrease of *Glud1* mRNA suggests that the excess glutamate was taken away from tricarboxylic acid (TCA) cycle anaplerosis and redirected into glutathione synthesis to protect hepatocytes from oxidative damage. Slowing of the TCA flux was also supported by the finding of an increased NAD^+/NADH ratio that further pointed out the inhibition of the activities of the TCA cycle dehydrogenases, leading to fumarate (Figure 4D) and citrate accumulation compared to

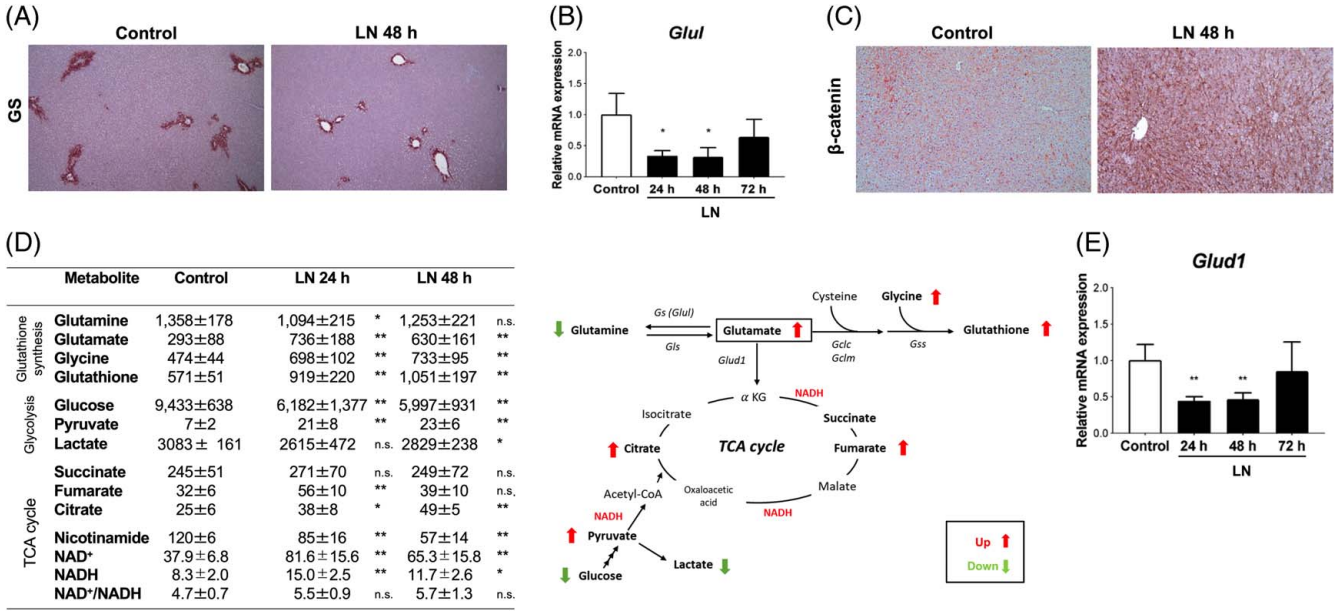

	Metabolite	Control	LN 24 h		LN 48 h	
Glutathione synthesis	Glutamine	1,358±178	1,094±215	*	1,253±221	n.s.
	Glutamate	293±88	736±188	**	630±161	**
	Glycine	474±44	698±102	**	733±95	**
	Glutathione	571±51	919±220	**	1,051±197	**
Glycolysis	Glucose	9,433±638	6,182±1,377	**	5,997±931	**
	Pyruvate	7±2	21±8	**	23±6	**
	Lactate	3083± 161	2615±472	n.s.	2829±238	*
TCA cycle	Succinate	245±51	271±70	n.s.	249±72	n.s.
	Fumarate	32±6	56±10	**	39±10	n.s.
	Citrate	25±6	38±8	*	49±5	**
	Nicotinamide	120±6	85±16	**	57±14	**
	NAD+	37.9±6.8	81.6±15.6	**	65.3±15.8	**
	NADH	8.3±2.0	15.0±2.5	**	11.7±2.6	*
	NAD+/NADH	4.7±0.7	5.5±0.9	n.s.	5.7±1.3	n.s.

FIGURE 4 LN affects glutamine metabolism. (A) IHC analysis of glutamine synthase (GS) (×10 magnification, (B) qRT-PCR analysis of *Glul,* and (C) IHC analysis of β-catenin (×10 magnification) in the liver of rats treated with LN. (D) Metabolome analysis of glycolysis, TCA cycle, and glutathione synthesis in the liver at 24 hours after LN. (E) qRT-PCR analysis of *Glud1* in the livers of LN-treated rats at 24, 48, and 72 hours. Relative mRNA expression was calculated using *Gapdh* as an endogenous control. Gene expression is reported as fold-change relative to livers from control rats. The graph bar represents mean values ± SD of 3 to 5 rats/group (*t* test). *$p < 0.05$ and **$p < 0.01$ compared to controls. n.s, not significant. Abbreviations: Gs, glutamine synthetase; Glud1, glutamate dehydrogenase 1; Glul, glutamate-ammonia ligase; LN, lead nitrate; T3, triiodothyronine; TCA, tricarboxylic acid cycle.

controls. Taken together, these results indicate that Nrf2 stimulates changes in glutamine metabolism.

LN targets OXPHOS through impairment of complex II of the electron transport chain

Metabolic reprogramming of preneoplastic and neoplastic hepatocytes is often associated with an impairment of OXPHOS.[13] To investigate whether LN affects OXPHOS in addition to the glucose and glutamine metabolism, we measured the content and activity of succinate dehydrogenase, the complex II of the respiratory chain.[33]

Histochemical analysis showed that the activity of succinate dehydrogenase was severely impaired in LN-treated livers at 24 and 48 hours compared to normal liver (Figure 5A). Biochemical measurements of the enzymatic activity of complex II confirmed the significant decrease caused by LN treatment (Figure 5B). These findings, together with the accumulation of fumarate at 24 hours (Figure 4D), point to a strong impairment of OXPHOS associated with the slowing of the TCA cycle flux in LN-treated rat livers.

LN increases proline biosynthesis

We next examined proline uptake and metabolism, as these are known to be upregulated in a variety of human cancers.[34] The enzymes involved in the proline biosynthesis, pyrrolidine-5-carboxylate reductase (Pycr1) and aldehyde dehydrogenase 18 family member A1 (Aldh18a1), are also overexpressed in most of these tumors, and the excess of glutamate is diverted to sustain proline biosynthesis.[34] As shown in Figure 5C, D, the expressions of *Aldh18a1* and *Pycr1* were strikingly induced by LN-treated rat livers at 24 hours, while proline dehydrogenase (*Prodh*) catalyzing the degradation of proline was significantly decreased at all-time points. However, metabolome analysis showed that proline content did not significantly change in LN-treated WT rats (Figure 5D), suggesting that the steady-state proline concentration must be a result of multiple regulations, as proline is involved in various metabolic pathways.

Nrf2 is essential for LN-induced hepatocyte proliferation

Since Nrf2 activation was observed in LN-treated rat livers, we investigated whether Nrf2 is essential for LN-induced hepatocyte proliferation. To this end, we first exploited brusatol (BR), a quassinoid isolated from the fruit of the Brucea javanica, which is widely used as an Nrf2 inhibitor.[35] A single-dose treatment with BR strikingly impaired LN-induced hepatocyte proliferation, assessed by BrdU uptake (Figure 6A). BrdU-positive hepatocyte nuclei were significantly increased by LN treatment, but this increase was almost completely abrogated by

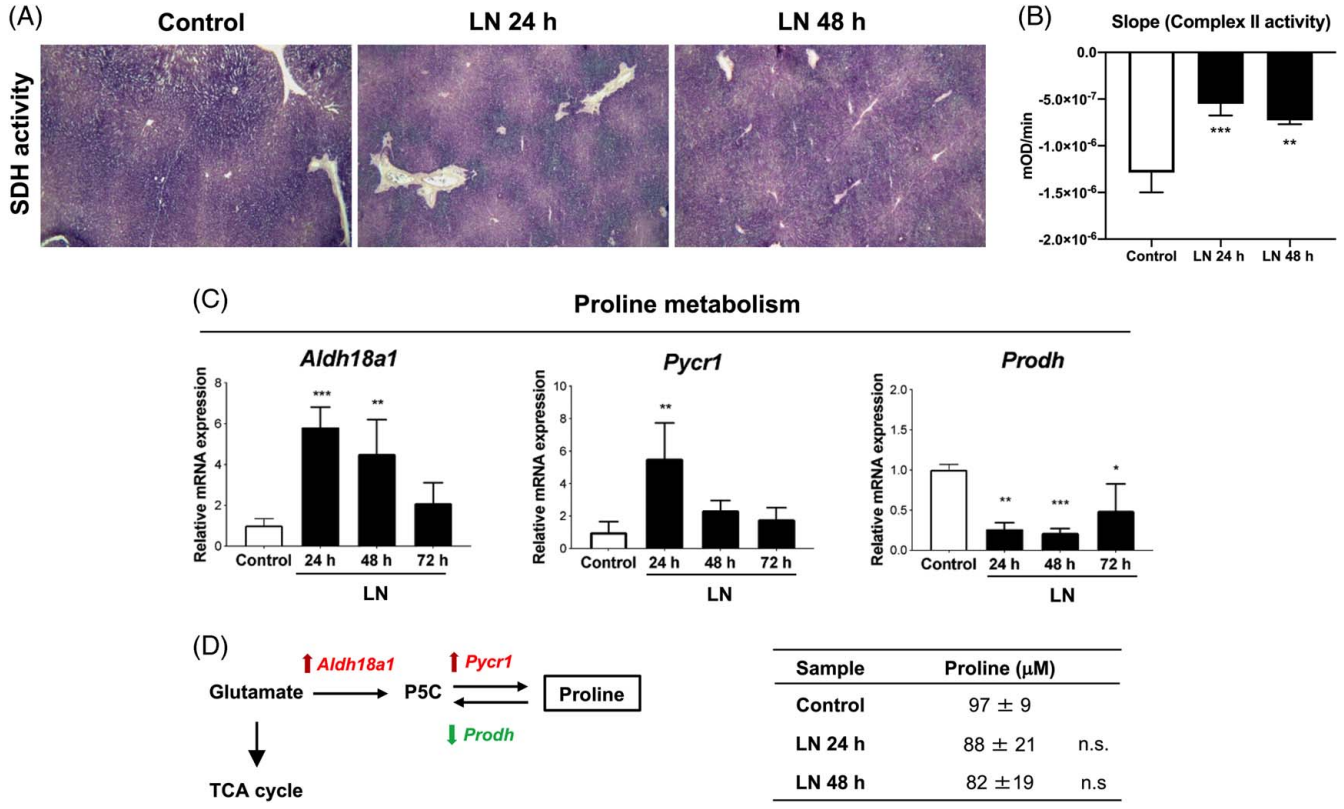

Sample	Proline (μM)	
Control	97 ± 9	
LN 24 h	88 ± 21	n.s.
LN 48 h	82 ±19	n.s

FIGURE 5 LN impairs oxidative phosphorylation while promoting proline biosynthesis. (A) Histochemical reaction evaluating hepatic succinate dehydrogenase activity in rat livers (×5 magnification) 24 and 48 after treatment with LN. (B) Complex II activity in the livers of rats 24 and 48 hours after treatment with LN (*t* test). $^{**}p < 0.01$ and $^{***}p < 0.001$ compared to control. (C) qRT-PCR analysis of *Pycr1*, *Aldh18a1*, and *Prodh* mRNA expression levels in the liver of control or LN-treated rats at 24, 48, and 72 hours. Relative mRNA expression was calculated using *Gapdh* as an endogenous control. Gene expression is reported as fold-change relative to livers from control rats. The histogram represents mean values ± SD of 5–6 rats/group (*t* test and ANOVA). $^{*}p < 0.05$, $^{**}p < 0.01$, and $^{***}p < 0.001$ compared to its own control. (D) Schematic representation of the effect of LN on proline biosynthesis. (E) Proline content in the liver of rats killed 24 and 48 hours after LN. Abbreviations: Aldh18a1, aldehyde dehydrogenase 18 family member A1; LN, lead nitrate; n.s, not significant; Prodh, proline dehydrogenase; Pycr1, pyrrolidine-5-carboxylate reductase; SDH, succinate dehydrogenase.

concomitant treatment with BR (Figure 6B). In agreement, BR partially reduced the LN-induced increase in liver weight (Figure 6C).

Since BR is an inhibitor of whole protein synthesis but not a specific Nrf2 inhibitor,[36,37] we took advantage of Nrf2 KO (F344-*Nfe2l2*^{em2Kyo}) rats[26] to directly investigate the role of Nrf2 in proliferation and metabolic reprogramming of normal hepatocytes. As shown in Figure 6D, in WT rats, mRNAs levels of Nrf2 targets, such as *Nqo1*, *Gstp1*, and *Gclc*, were significantly increased 24 hours after LN, while *Nrf2* gene knockout strongly abrogated the increase of mRNA levels (Figure 6D). Genetic knockout of Nrf2 also blunted LN-induced liver enlargement (Supplemental Figure S2A, http://links.lww.com/HEP/I7) in the absence of any clear evidence of hepatocyte damage (Supplemental Figure S2B, http://links.lww.com/HEP/I7).

Most importantly, while LN-treated WT rats exhibited a strong proliferative response, as detected by BrdU incorporation, practically, no hepatocyte proliferation was observed in the livers of Nrf2 KO rats (Figure 6E). Indeed, only nonparenchymal cells were BrdU-positive in the livers of Nrf2 KO rats. Quantification of BrdU-positive hepatocyte nuclei confirmed that the significant increase by LN treatment of BrdU hepatocyte nuclei was totally abrogated in the Nrf2 KO rat livers (Figure 6F). These results unequivocally demonstrate that Nrf2 is required for LN-induced hepatocyte proliferation. Conversely, when hepatocyte proliferation was triggered by T3, a liver mitogen that does not activate Nrf2, the genetic loss of Nrf2 did not influence the number of BrdU-positive cells (Supplemental Figure S2C, http://links.lww.com/HEP/I7).

Nrf2 is essential for LN-mediated metabolic reprogramming of normal hepatocytes

Since the genes responsible for glucose and glutamine metabolism induced by LN treatment in normal hepatocytes are under the transcriptional control of Nrf2, we investigated whether the LN-induced metabolic reprogramming could be affected by the genetic loss of Nrf2.

qRT-PCR analysis showed that the expression of mRNAs encoding enzymes involved in the oxidative

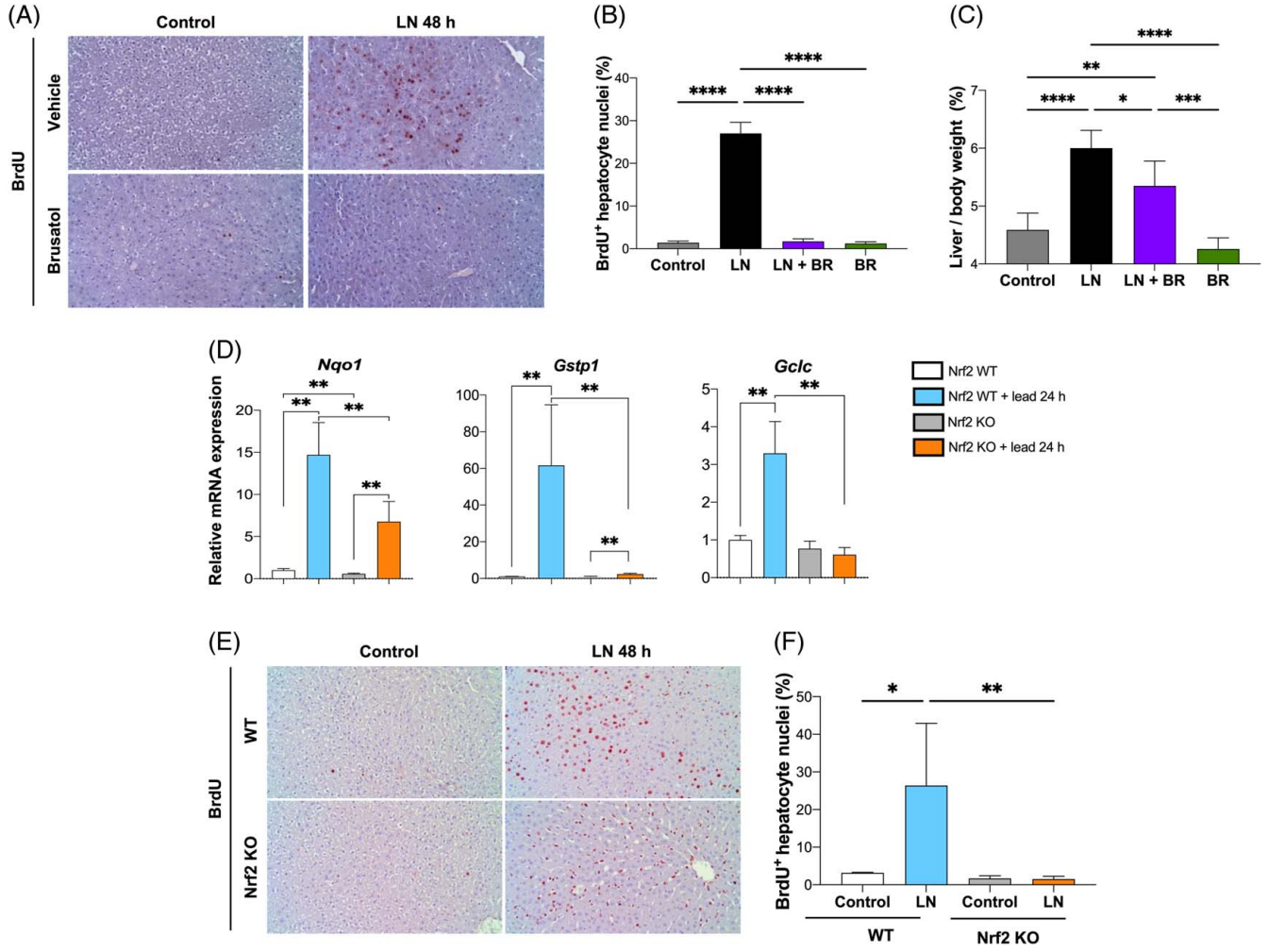

FIGURE 6 Nrf2 is required for LN-induced hepatocyte proliferation. (A) Microphotograph illustrating several BrdU-positive nuclei of hepatocytes in the liver of rats 48 hours after treatment with LN. Virtually no BrdU-positive hepatocytes are observed in the liver of rats treated with LN + Brusatol (BR) (×20 magnification). (B) Labeling index (LI) of hepatocyte nuclei and (C) relative liver weight 48 hours after treatment with LN or LN + BR. BrdU (1 mg/mL) dissolved in drinking water was given 2 hours after LN treatment. LI was expressed as the number of BrdU-positive hepatocyte nuclei/100 nuclei. *$p <$ 0.05, ***$p < 0.001$, and ****$p < 0.0001$. (D) qRT-PCR analysis of representative Nrf2 target genes such as *Nqo1*, *Gstp1,* and *Gclc* mRNA levels 24 hours after treatment of WT and KO rats with LN. Relative mRNA expression was calculated using *Gapdh* as an endogenous control. Gene expression is reported as fold-change relative to livers from untreated controls. The graph bars represent mean values ± SD of 5–6 rats/group (ANOVA). **$p < 0.01$ compared to controls. (E) Microphotograph illustrating several BrdU-positive nuclei of hepatocytes in the liver of WT rats 48 hours after treatment with LN (×20 magnification). Only nonparenchymal cells are BrdU-positive in the liver of LN-treated Nrf2 KO rats. (F) LI was expressed as the number of BrdU-positive hepatocyte nuclei/100 nuclei. The graph bars represent mean values ± SD of 4–7 rats/group (ANOVA). *$p < 0.05$. **$p < 0.01$. Abbreviations: BR, brusatol; BrdU, bromodeoxyuridine; Gclc, glutamate-cysteine ligase catalytic subunit; Gstp1, placental glutathione S-transferase; LN, lead nitrate; Nqo1, NAD(P)H quinone dehydrogenase 1; Nrf2, nuclear factor (erythroid-derived 2)-like 2; KO, knockout; WT, wild-type.

branch of the PPP, for example, *G6pd* and *Pgd*, as well as in the nonoxidative branch, for example, *Tkt,* was significantly increased in LN-treated WT rats, while expression of these genes was markedly reduced in Nrf2 KO rat livers (Figure 7A). This expression profile closely resembles that of the major Nrf2 target genes encoding detoxifying and antioxidant proteins (Figure 6C–E). IHC analysis confirmed the induction of G6PD, NQO1, and GSTP protein levels in LN-treated WT rats, which was abrogated in Nrf2 KO rats (Figure 7B).

We also examined the expression of additional genes encoding for NADPH-generating enzymes, such as malic enzyme 1 (*Me1*) and isocitrate dehydrogenase 1 (*Idh1*), known to contribute to NADPH/NADP balance within the cell and general redox homeostasis. Similar to PPP-related genes (Figure 7A), the expression of *Me1*, an Nrf2 target gene,[38] was upregulated in LN-treated WT rats but not in Nrf2 KO rats (Figure 7C). On the contrary, *Idh1,* was induced by LN treatment but was not influenced by loss of Nrf2 (Figure 7C).

When we investigated the expression of genes linked to glutamine metabolism, we found that *Glul* mRNA was significantly decreased in LN-treated WT rats, while this repression was almost completely abrogated by Nrf2 KO (Figure 7D). Conversely, *Gls* mRNA was not affected by LN treatment in WT rats, but the *Gls* expression

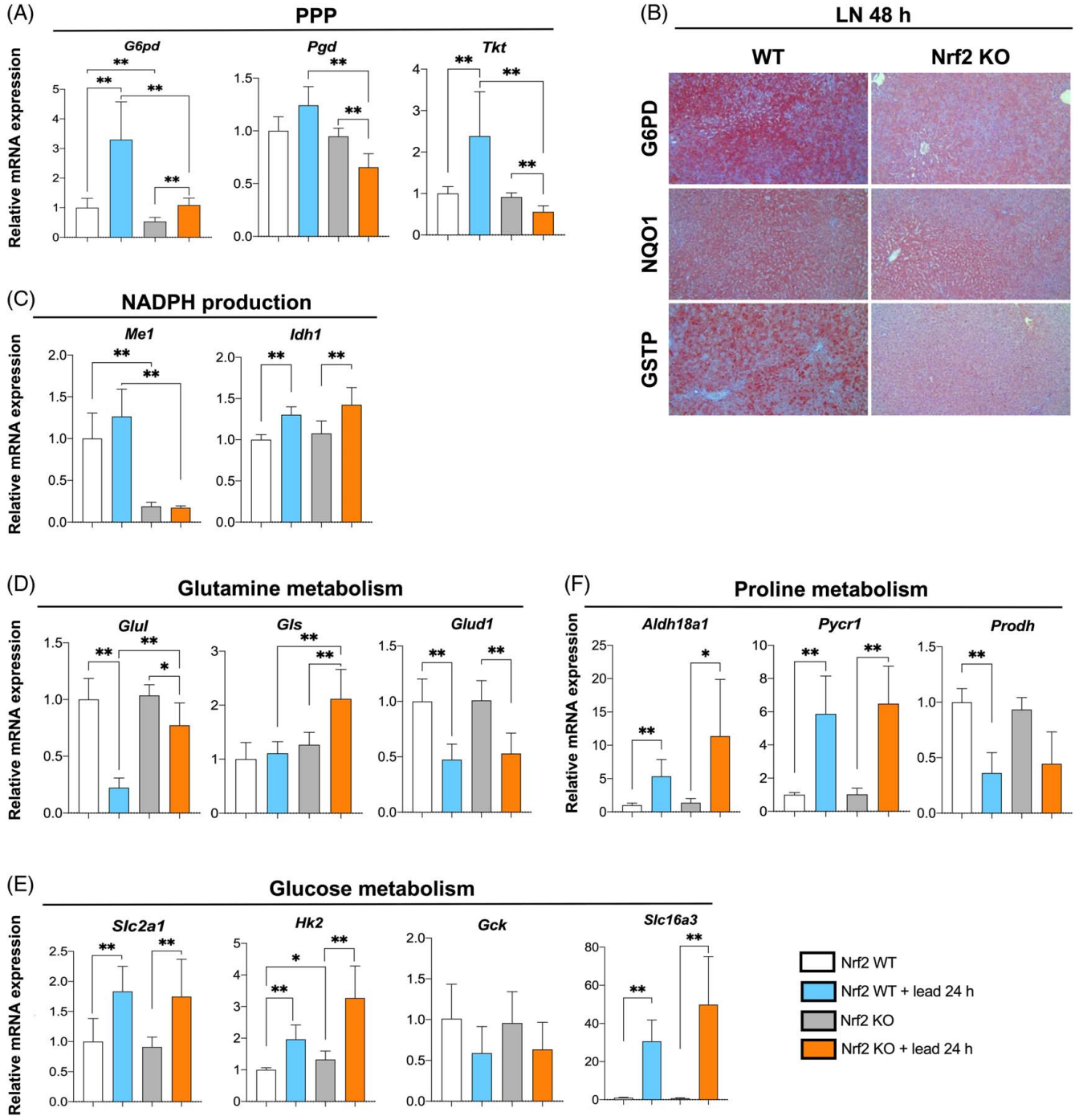

FIGURE 7 Nrf2 is required for the activation of the oxidative brunch of PPP and glutamine metabolism following LN administration. (A) qRT-PCR analysis of mRNA levels of genes involved in PPP (*G6pd*, *Pgd*, and *Tkt*) in the livers of WT and Nrf2 KO rats treated with LN. (B) IHC analysis of G6PD, GSTP, and NQO1 (×10 magnification). (C) qRT-PCR analysis of mRNA levels of genes involved in NADPH production (*Me1*, *Idh1*). (D) in glutamine metabolism (*Glul*, *Gls*, and *Glud1*). (E) In glucose metabolism (*Slc2a1*, *Gck*, *Hk2*, and *Slc16a3)*. Relative mRNA expression was calculated using *Gapdh* as an endogenous control. Gene expression is reported as fold-change relative to livers from untreated rats. The histogram represents mean values ± SD of 5–6 rats/group (*t* test and ANOVA). $*p < 0.05$ and $**p < 0.01$. Abbreviations: Aldh18a1, aldehyde dehydrogenase 18 family member A1; G6PD, glucose-6-phosphate dehydrogenase; Glud1, glutamate dehydrogenase 1; Glul, glutamate-ammonia ligase; Gstp, placental glutathione S-transferase; KO, knockout; LN, lead nitrate; Me1, malic enzyme 1; Nqo1, NAD(P)H quinone dehydrogenase 1; Nrf2, nuclear factor (erythroid-derived 2)-like 2; Pgd, phosphogluconate dehydrogenase; PPP, pentose phosphate pathway; Prodh, proline dehydrogenase; Pycr1, pyrrolidine-5-carboxylate reductase; T3, triiodothyronine; WT, wild-type.

increased 2-fold following LN treatment in Nrf2 KO rats (Figure 7D). Similar to the expression profile of *Glul*, *Glud1* mRNA expression was markedly decreased by the LN treatment. However, this decrease was not abrogated by Nrf2 KO (Figure 7D). These results indicate that the expressions of glutamine metabolism-

related genes are under multiple regulations. Thus, while Nrf2 markedly influences these genes, it could only partially explain the metabolic reprogramming exerted by LN treatment.

Regarding the genes associated with glycolysis, LN treatment significantly increased the expression levels of *Slc2a1*, *Slc16a3*, and *Hk2* whereas reduced those of *Gck* (Figure 7E). However, we found no major difference in the expression of these genes between LN-treated WT and Nrf2 KO rats, suggesting that Nrf2 may not contribute substantially to the glycolytic pathway. Similarly, when we examined the genes involved in proline synthesis (such as *Pycr1* and *Aldh18a1*) or proline degradation (such as *Prodh*), upon LN administration, we found no differential effect in Nrf2 KO animals (Figure 7F). Taken together, the gene expression profile analyzed upon NRF2 KO indicated that the NRF2-dependent LN-mediated proliferation in hepatocytes is potentially ascribed to positive regulation of the PPP.

Nrf2 is essential for the LN-mediated increase of glutathione and glycine

To examine whether and how the changes in gene expression profiles influence the metabolic reprogramming of LN-treated rats, we subjected WT and Nrf2 KO rat livers to NMR-based metabolomics. Particularly, informed by the gene expression data, metabolites responsible for glycolysis, PPP, glutaminolysis, and amino acid metabolism were monitored in 24- and 48-hour LN- or T3-treated livers from WT and Nrf2 KO rats.

A supervised heatmap of the 54 analyzed metabolites derived from the livers of LN-treated WT and Nrf2 KO rats showed no major differences between the metabolites from untreated WT and Nrf2 KO livers (Figure 8A). However, a significant difference was found between metabolites derived from LN-treated WT and KO rats. Indeed, a strong decrease in metabolite content—particularly evident 24 hours after treatment—was observed in Nrf2 KO livers. Of the 54 metabolites, we further followed up on those related to the reactions catalyzed by the enzymes for which we analyzed the expression profile (Figure 8B–F).

Interestingly, among many LN-dependent metabolic changes, those involving the metabolisms of glutathione (Figure 8B), glucose (Figure 8C), TCA cycle (Figure 8D), NADH (Figure 8E), and nucleic acid synthesis (Figure 8F) were both LN- and Nrf2-dependent. A remarkable difference between the 2 groups was also observed in amino acid metabolisms, including glutamine and proline (Supplemental Figure S3, http://links.lww.com/HEP/I8). In comparison, no major change in metabolite content was observed in T3-treated WT compared to T3-treated Nrf2 KO rats (Figure 8B–F), further supporting our gene expression analyses showing a lack of metabolic reprogramming due to the inability of T3 to activate the Keap1-Nrf2 system. Furthermore, the striking enhancement of serine synthesis in rats treated with LN for 24 and 48 hours suggests its promoting effect on glycine availability for glutathione synthesis,[39] confirming the notion that most glutamate and glycine in our model could be redirected toward glutathione synthesis (Supplemental Figure S3, http://links.lww.com/HEP/I8).

Overall, the metabolome data suggests that Nrf2 redirects glutamate to glutathione synthesis, reducing the amount used to fuel the TCA cycle and mitochondrial activity, as proposed in other experimental conditions.[40] Despite the inhibitory effect of LN on glutamine synthesis, the metabolome analysis did not show major differences in glutamine content compared to controls, suggesting that glutamine content could be mainly derived by extracellular uptake.

DISCUSSION

One of the most described metabolic rewiring associated with neoplastic transformation is aerobic glycolysis (also known as the Warburg effect). This reprogramming occurs when glucose is not a limiting nutrient and allows cancer cells to enhance the levels of glycolytic intermediates, which are fundamental for anaplerotic reactions, including G6P that fuels the PPP, a pathway essential in providing reductive potential and pentoses. In such metabolic reprogramming, lactate secretion, ATP production, and amino acid synthesis are also often altered. This metabolic reprogramming has been observed in many cancers, including HCC, but it is unclear whether it is a unique property of neoplastic cells or if it takes place also in differentiated proliferating cells, such as hepatocytes; indeed, some of the metabolic dependencies of neoplastic cells, including aerobic glycolysis, have been observed also in rapidly proliferating cells, such as those involved in immunity, angiogenesis, pluripotency, and infection;[41,42] a remarkable example of this reprogramming in non-cancerous cells is the high glycolytic flux coupled with lower mitochondrial respiration in proliferating endothelial cells during angiogenesis.[43] These observations suggest that the Warburg effect operates in rapidly dividing cells in normal and/or pathological states other than neoplasia. Accordingly, some authors have defined glycolysis as a “hallmark of rapid proliferation” based on the assumption that rapidly proliferating cells seem to rely on aerobic glycolysis.[41] The advantage of exploiting aerobic glycolysis is also in the fraction of glucose-6-phosphate that could be diverted into the PPP. PPP is essential for providing NADPH for anabolic purposes and pentoses for DNA and RNA synthesis. A major transcription factor that can directly control the PPP flux is NRF2.

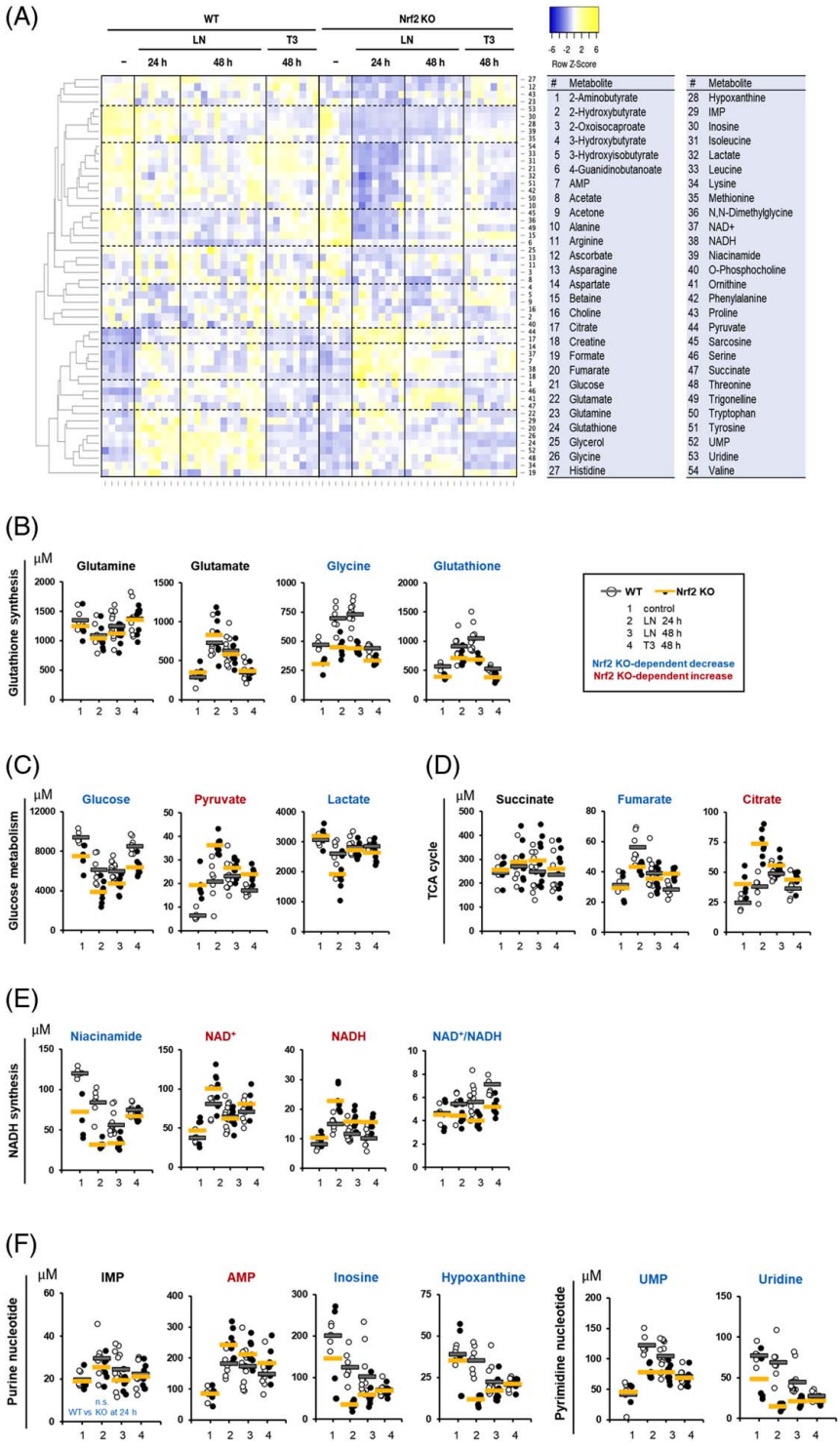

FIGURE 8 NMR metabolites in the liver of WT and Nrf2 KO rats treated with LN. (A) Heatmap analysis showing metabolites intensity. The row and column represent a metabolite feature and a sample, respectively. The row Z-score or scaled expression value of each feature is plotted in a yellow-blue color scale. The yellow and blue of the tile indicate high and low abundance, respectively. Altered metabolites involved in glutathione synthesis (B), glucose metabolism (C), TCA cycle (D), NADH synthesis (E), and purine and pyrimidine nucleotide synthesis (F). Abbreviations: IMP, inosine monophosphate; KO, knockout; LN, lead nitrate; Nrf2, nuclear factor (erythroid-derived 2)-like 2; UMP, uridine monophosphate; WT, wild-type.

This study deepens this scientific debate and demonstrates *in vivo* experimental models characterized by a synchronous and rapid proliferation of well-differentiated nonneoplastic hepatocytes that: (1) neither Nrf2 activation nor the Warburg effect is a *sine qua non* condition to trigger cell proliferation, as shown by the lack of increased glycolysis in proliferating cells upon T3 or PH; (2) metabolic reprogramming, namely, a switch from

OXPHOS to glycolysis, PPP activation, altered glutamine metabolism, and increased proline biosynthesis, takes place in normal proliferating hepatocytes under certain environmental conditions, such as LN treatment; and (3) similar to what observed in cancer cells,[7] Nrf2 activation is required for PPP activation and promotion of proliferation of fully differentiated hepatocytes following LN treatment. Thus, opposite to common belief, transient activation of Nrf2 confers normal hepatocytes a highly specialized metabolism by reducing reactive oxygen species production from mitochondrial metabolism, enhancing NADPH availability through G6pd, and favoring glutathione synthesis, essential for the potent antioxidant and detoxification capacities usually displayed by cancer cells.

Regarding hepatocyte proliferation, the lack of increased expression of several Nrf2 target genes in the liver of rats treated with T3 or subjected to PH clearly shows that it can occur in the absence of Nrf2 activation, indicating that activation of this transcription factor is not an essential requirement for the entry of normal hepatocytes into the cell cycle. In addition, following T3 or PH, rapidly proliferating hepatocytes showed neither evidence of the Warburg effect nor induction of G6pd, the rate-limiting enzyme of PPP. However, while these findings seem to support the notion that Nrf2 activation leading to the Warburg effect and PPP activation is exclusive of cancer cells, a strong Nrf2 activation and features of metabolic reprogramming almost identical to that often seen in tumors were observed in LN-induced hepatocyte proliferation. Indeed, enhanced uptake of glucose accompanied by PPP activation was found following treatment with LN, probably representing an adaptive cellular response to OXPHOS failure consequent to the metabolic impairment of the mitochondrial complexes caused by LN.

Notably, the metabolic switch seen in LN-treated rats preceded hepatocyte proliferation and was associated with a massive activation of Nrf2 due, at least in part, to p62 accumulation and phosphorylation, a condition known to favor Nrf2 nuclear translocation and transcriptional activation.

Metabolomics analysis of livers from LN-treated rats highlighted a decrease in glutamine synthesis compared to the control liver, concomitant with a striking increase in glutamate and glycine levels. The significant decrease of *Glud1* mRNA, paralleled by enhanced expression of *Gclc*, suggested that the excess of glutamate was removed from the TCA cycle and redirected into glutathione synthesis to protect hepatocytes from oxidative damage. Furthermore, our results also highlighted enhanced proline biosynthesis—a central downstream metabolic pathway largely supplied by glutamate[34]—in LN-treated rat livers. Indeed, *Aldh18a1* and *Pycr1*, the genes encoding for the 2 enzymes operating proline biosynthesis and overexpressed in most human tumors, including HCC, were overexpressed following LN treatment. Overall, we conclude that the metabolic features observed after LN almost entirely recapitulate what is observed in human HCC induced by oncogenes, such as c-Myc, or in preneoplastic and neoplastic lesions induced by chemical carcinogens.[13,44]

However, contrary to our expectations, LN was effective also in $Nrf2^{-/-}$ rats in altering the glycolytic-related metabolites and the expression levels of glycolytic enzymes, as well as those involved in glutamine and proline metabolism. Together, these data suggest that most metabolic changes are consequent to LN treatment and are not Nrf2-dependent.

Nevertheless, the critical role played by Nrf2 in the induction of "cancer-like" metabolic reprogramming is evident by the lack of PPP activation in $Nrf2^{-/-}$ rats. While this observation *per se* is not surprising, since many genes involved in PPP are well-known Nrf2 targets, it is remarkable that lack of PPP activation resulted in an almost complete impairment of hepatocyte proliferation in LN-treated rats. In this context, It should be stressed that, while induction of G6pd is not mandatory during the proliferation of normal hepatocytes (ie, after T3 or PH), mounting evidence suggests that it is overexpressed in many experimental and human cancers, and its expression is associated with cancer progression and poor prognosis in many tumor types, including HCC.[45,46] These results further support previous findings suggesting the critical role of Nrf2 in redirecting glucose metabolism toward the anabolic metabolism of cancer cells.

A relevant finding stemming from our work is that, in agreement with Chan et al[47], in a different experimental setting and in a different species (mice vs. rats), NRF2 is a master gene in the control of hepatocyte proliferation, and thus, its induction can be seen as a promising approach to improve liver regeneration in pathological conditions, such as post-hepatectomy liver failure.

We believe that another added value of our work is the fact that it offers a rapid and useful *in vivo* model to study the molecular alterations underpinning the differences/similarities of metabolic changes in normal and neoplastic hepatocytes. In this context, identification of the metabolic dependencies of HCC and the comparison with those of normal proliferating differentiated hepatocytes may help identify metabolic vulnerabilities that could be exploited to design molecules to be used for therapeutic strategies.

AUTHOR CONTRIBUTIONS

Amedeo Columbano and Masayuki Yamamoto: conceptualization, data curation, funding acquisition, supervision, writing—original draft, writing—review and editing. Silvia Giordano: conceptualization, funding acquisition, supervision, writing—original draft; Marta A. Kowalik and Keiko Taguchi: conceptualization, data curation, funding acquisition, writing—original draft, writing—review and

editing. Elisabetta Puliga: methodology, data curation. Andrea Perra: data curation, methodology. Andrea Caddeo: methodology, data curation, writing—review and editing. Marina Serra: methodology, data curation, writing—review and editing. Andrea Morandi: methodology, data curation, funding acquisition, writing—original draft, writing—review and editing. Marina Bacci: methodology, data curation. Seizo Koshiba, Jin Inoue, and Eiji Hishinuma: methodology, data curation.

FUNDING INFORMATION

This research was funded by Associazione Italiana Ricerca sul Cancro (AIRC), Grant IG-20176 to AC; MEXT/JSPS KAKENHI 19H05649 to Masayuki Yamamoto and 22K06906 to Keiko Taguchi; Grant IG-27531 to Silvia Giordano; and Grant IG-22941 to Andrea Morandi.

CONFLICTS OF INTEREST

The authors have no conflicts to report.

REFERENCES

1. Hanahan D, Weinberg RA. The hallmarks of cancer. Cell. 2000; 100:57–70.
2. Hanahan D. Hallmarks of cancer: new dimensions. Cancer Discov. 2022;12:31–46.
3. Warburg O. On the origin of cancer cells. Science. 1956;123: 309–14.
4. Pavlova NN, Thompson CB. The emerging hallmarks of cancer metabolism. Cell Metab. 2016;23:27–47.
5. Motohashi H, Yamamoto M. Nrf2-Keap1 defines a physiologically important stress response mechanism. Trends Mol Med. 2004;10:549–7.
6. Rojo de la Vega M, Chapman E, Zhang DD. NRF2 and the hallmarks of cancer. Cancer Cell. 2018;34:21–43.
7. Mitsuishi Y, Taguchi K, Kawatani Y, Shibata T, Nukiwa T, Aburatani H, et al. Nrf2 redirects glucose and glutamine into anabolic pathways in metabolic reprogramming. Cancer Cell. 2012;22:66–79.
8. Menegon S, Columbano A, Giordano S. The dual roles of NRF2 in cancer. Trends Mol Med. 2016;22:578–93.
9. Sung H, Ferlay J, Siegel RL, Laversanne M, Soerjomataram I, Jemal A, et al. Global Cancer Statistics 2020: GLOBOCAN estimates of incidence and mortality worldwide for 36 cancers in 185 countries. CA Cancer J Clin. 2021;71:209–49.
10. Guichard C, Amaddeo G, Imbeaud S, Ladeiro Y, Pelletier L, Maad IB, et al. Integrated analysis of somatic mutations and focal copy-number changes identifies key genes and pathways in hepatocellular carcinoma. Nat Genet. 2012;44:694–8.
11. Cleary SP, Jeck WR, Zhao X, Chen K, Selitsky SR, Savich GL, et al. Identification of driver genes in hepatocellular carcinoma by exome sequencing. Hepatology. 2013;58:1693–702.
12. Totoki Y, Tatsuno K, Covington KR, Ueda H, Creighton CJ, Kato M, et al. Trans-ancestry mutational landscape of hepatocellular carcinoma genomes. Nat Genet. 2014;46:1267–73.
13. Kowalik MA, Guzzo G, Morandi A, Perra A, Menegon S, Masgras I, et al. Metabolic reprogramming identifies the most aggressive lesions at early phases of hepatic carcinogenesis. Oncotarget. 2016;7:32375–93.
14. Kowalik MA, Puliga E, Cabras L, Sulas P, Petrelli A, Perra A, et al. Thyroid hormone inhibits hepatocellular carcinoma progression via induction of differentiation and metabolic reprogramming. J Hepatol. 2020;72:1159–69.
15. Beyer TA, Xu W, Teupser D, auf dem Keller U, Bugnon P, Hildt E, et al. Impaired liver regeneration in Nrf2 knockout mice: role of ROS-mediated insulin/IGF-1 resistance. EMBO J. 2008;27: 212–3.
16. Shirasaki K, Taguchi K, Unno M, Motohashi H, Yamamoto M. NF-E2-related factor 2 promotes compensatory liver hypertrophy after portal vein branch ligation in mice. Hepatology. 2014;59: 2371–82.
17. Higgins G, Anderson RE. Experimental pathology of liver: restoration of liver in white rat following partial surgical removal. 1931.
18. Michalopoulos GK. Liver regeneration after partial hepatectomy: critical analysis of mechanistic dilemmas. Am J Pathol. 2010; 176:2–13.
19. Köhler UA, Kurinna S, Schwitter D, Marti A, Schäfer M, Hellerbrand C, et al. Activated Nrf2 impairs liver regeneration in mice by activation of genes involved in cell-cycle control and apoptosis. Hepatology. 2014;60:670–8.
20. Hu M, Zou Y, Nambiar SM, Lee J, Yang Y, Dai G. Keap1 modulates the redox cycle and hepatocyte cell cycle in regenerating liver. Cell Cycle. 2014;13:2349–58.
21. Karp SJ. Clinical implications of advances in the basic science of liver repair and regeneration. Am J Transplant. 2009;9:1973–80.
22. Columbano A, Shinozuka H. Liver regeneration versus direct hyperplasia. FASEB J. 1996;10:1118–28.
23. Shinozuka H, Kubo Y, Katyal SL, Coni P, Ledda-Columbano GM, Columbano A, et al. Roles of growth factors and of tumor necrosis factor-alpha on liver cell proliferation induced in rats by lead nitrate. Lab Invest. 1994;71:35–41.
24. Ledda-Columbano GM, Columbano A, Cannas A, Simbula G, Okita K, Kayano K, et al. Dexamethasone inhibits induction of liver tumor necrosis factor-alpha mRNA and liver growth induced by lead nitrate and ethylene dibromide. Am J Pathol. 1994;145: 951–8.
25. Columbano A, Ledda-Columbano GM, Ennas MG, Curto M, Chelo A, Pani P. Cell proliferation and promotion of rat liver carcinogenesis: different effect of hepatic regeneration and mitogen induced hyperplasia on the development of enzyme-altered foci. Carcinogenesis. 1990;11:771–6.
26. Taguchi K, Takaku M, Egner PA, Morita M, Kaneko T, Mashimo T, et al. Generation of a new model rat: Nrf2 knockout rats are sensitive to aflatoxin B1 toxicity. Toxicol Sci. 2016;152:40–52.
27. Koshiba S, Motoike I, Saigusa D, Inoue J, Shirota M, Katoh Y, et al. Omics research project on prospective cohort studies from the Tohoku Medical Megabank Project. Genes Cells. 2018;23: 406–17.
28. Komatsu M, Kurokawa H, Waguri S, Taguchi K, Kobayashi A, Ichimura Y, et al. The selective autophagy substrate p62 activates the stress responsive transcription factor Nrf2 through inactivation of Keap1. Nat Cell Biol. 2010;12:213–23.
29. Ichimura Y, Waguri S, Sou Y, Kageyama S, Hasegawa J, Ishimura R, et al. Phosphorylation of p62 activates the Keap1-Nrf2 pathway during selective autophagy. Mol Cell. 2013;51: 618–31.
30. Loeppen S, Schneider D, Gaunitz F, Gebhardt R, Kurek R, Buchmann A, et al. Overexpression of glutamine synthetase is associated with beta-catenin-mutations in mouse liver tumors during promotion of hepatocarcinogenesis by phenobarbital. Cancer Res. 2002;62:5685–8.
31. Mattu S, Saliba C, Sulas P, Zavattari P, Perra A, Kowalik MA, et al. High frequency of β-catenin mutations in mouse hepatocellular carcinomas induced by a nongenotoxic constitutive androstane receptor agonist. Am J Pathol. 2018;188:2497–507.
32. Li M, Chiu J-F, Kelsen A, Lu SC, Fukagawa NK. Identification and characterization of an Nrf2-mediated ARE upstream of the rat glutamate cysteine ligase catalytic subunit gene (GCLC). J Cell Biochem. 2009;107:944–54.
33. Cecchini G. Function and structure of complex II of the respiratory chain. Annu Rev Biochem. 2003;72:77–109.

34. Ding Z, Ericksen RE, Escande-Beillard N, Lee QY, Loh A, Denil S, et al. Metabolic pathway analyses identify proline biosynthesis pathway as a promoter of liver tumorigenesis. J Hepatol. 2020; 72:725–35.
35. Ren D, Villeneuve NF, Jiang T, Wu T, Lau A, Toppin HA, et al. Brusatol enhances the efficacy of chemotherapy by inhibiting the Nrf2-mediated defense mechanism. Proc Natl Acad Sci USA. 2011;108:1433–8.
36. Vartanian S, Ma TP, Lee J, Haverty PM, Kirkpatrick DS, Yu K, et al. Application of mass spectrometry profiling to establish brusatol as an inhibitor of global protein synthesis. Mol Cell Proteomics. 2016;15:1220–31.
37. Harder B, Tian W, La Clair JJ, Tan AC, Ooi A, Chapman E, et al. Brusatol overcomes chemoresistance through inhibition of protein translation. Mol Carcinog. 2017;56:1493–500.
38. Lee J-M, Calkins MJ, Chan K, Kan YW, Johnson JA. Identification of the NF-E2-related factor-2-dependent genes conferring protection against oxidative stress in primary cortical astrocytes using oligonucleotide microarray analysis. J Biol Chem. 2003;278:12029–38.
39. Yang M, Vousden KH. Serine and one-carbon metabolism in cancer. Nat Rev Cancer. 2016;16:650–2.
40. Sayin VI, LeBoeuf SE, Singh SX, Davidson SM, Biancur D, Guzelhan BS, et al. Activation of the NRF2 antioxidant program generates an imbalance in central carbon metabolism in cancer. Elife. 2017;6:e28083.
41. Abdel-Haleem AM, Lewis NE, Jamshidi N, Mineta K, Gao X, Gojobori T. The emerging facets of non-cancerous Warburg effect. Front Endocrinol (Lausanne). 2017;8:279.
42. Pouysségur J, Marchiq I, Parks SK, Durivault J, Ždralević M, Vucetic M. "Warburg effect" controls tumor growth, bacterial, viral infections and immunity - Genetic deconstruction and therapeutic perspectives. Semin Cancer Biol. 2022;86:334–46.
43. De Bock K, Georgiadou M, Schoors S, Kuchnio A, Wong BW, Cantelmo AR, et al. Role of PFKFB3-driven glycolysis in vessel sprouting. Cell. 2013;154:651–3.
44. Yuneva MO, Fan TWM, Allen TD, Higashi RM, Ferraris DV, Tsukamoto T, et al. The metabolic profile of tumors depends on both the responsible genetic lesion and tissue type. Cell Metab. 2012;15:157–70.
45. Kowalik MA, Columbano A, Perra A. Emerging role of the pentose phosphate pathway in hepatocellular carcinoma. Front Oncol. 2017;7:87.
46. Patra KC, Hay N. The pentose phosphate pathway and cancer. Trends Biochem Sci. 2014;39:347–54.
47. Chan BKY, Elmasry M, Forootan SS, Russomanno G, Bunday TM, Zhang F, et al. Pharmacological activation of Nrf2 enhances functional liver regeneration. Hepatology. 2021;74:973–86.

How to cite this article: Kowalik MA, Taguchi K, Serra M, Caddeo A, Puliga E, Bacci M, et al. Metabolic reprogramming in Nrf2-driven proliferation of normal rat hepatocytes. Hepatology. 2024;79:829–843. https://doi.org/10.1097/HEP.0000000000000568